Nanofibrous Material of N-Succinyl Chitosan/ Polyethylene Oxide in the Removal of Emerging Pharmaceuticals from Aqueous Solution by Adsorption/Desorption Method

Amna Hassan Issa Khierallah,[a,*] Amel Hadj Bouazza,[b] and Daniel Montplaisir [c]

Pharmaceutical metabolites and their residues have been identified as major environmental pollutants in aquatic ecosystems. N-succinyl chitosan (NSCS) was studied as a potential adsorbent for a pharmaceutical residue, fluoxetine, from aqueous media. NSCS was investigated using Fourier transform infrared (FTIR) and ^{1}H-nuclear magnetic residence (NMR) spectroscopies. Scanning electron microscopy (SEM) was used to investigate the formation of nanofibers by electrospinning of these green biomaterial polymer membranes. The mechanisms of FLX adsorption, as well as the effects of pH value in the original solution on adsorption capacities, were investigated using high-performance liquid chromatography (HPLC-UV DAD) under identical adsorption conditions. It was found that NSCS/PEO nanofibers with a diameter of 183 ± 38 nm were more effective to remove pharmaceutical residues from aqueous media than other commercial and modified adsorbents such as activated carbon (AC). FLX adsorption on NSCS/PEO nanofibers was favoured at pH 8.0. Pseudo-first order model was the more adequate to represent the kinetic data, being the maximum adsorption capacities of FLX on NSCS/PEO reached up to 70%. A study of the desorption potential and reusability of the mat was also conducted. According to the results, electrospun NSCS/PEO mats can be desorption and reused up to 4 times without significant loss in adsorption capability.

DOI: 10.15376/biores.18.1.1971-1998

Keywords: Wastewater treatment; N-Succinyl Chitosan; Pharmaceutical residues; Electrospinning; Nanofibers; Adsorption/Desorption.

Contact information: a: Institut d'Innovations en Écomatériaux, Écoproduits et Écoénergies (I2E3), Université du Québec à Trois-Rivières, Trois-Rivières (QC), Canada; b: Inovem, 765, rue Notre-Dame Est, Victoriaville, Qc, CA G6P 4B2; c: Department of Chemistry, Biochemistry and Physics, Université du Québec à Trois-Rivières, Trois Rivières (QC), Canada; Corresponding author: amna.khierallah@uqtr.ca

INTRODUCTION

Water is an essential natural resource that is utilized at a global scale at a rate of billions of cubic metres each year. A world without water would be a lifeless planet. It is critical to conduct research on its use and protection in order to create new ways and materials for maintaining water quality (Howard and Bartram 2010). Water contamination causes deaths and illnesses all over the globe, and roughly 14,000 people die as a result of it every day (Chaudhry and Malik 2017). Chemicals that are not routinely monitored or regulated in the environment are known as emerging contaminants (ECs) (Erickson *et al*. 2014). There are various categories of such chemicals. Prescription and over-the-counter medications, fire retardants, insecticides, hormones, detergents, and personal care products

are a few examples. Based on studies showing their presence in treated wastewater and in surface and drinking water, pharmaceuticals, and personal care products (PPCPs) have been identified as developing contaminants of concern (Ebele *et al*. 2017a). There are several problems identified with health and the environment that are caused by urban effluents, and the ever-complicated drainage systems add to the complex disposal methods that are highly expensive (Hernandez-Ramirez and Holmes 2008). The vast volumes of waste generated by residential and industrial use make it impracticable to apply this method. Consequently, there is a need to find low-cost cleaning procedures to resolve these challenges (Ferronato and Torretta 2019). To solve some of the identified environmental challenges, less expensive adsorbents derived from electrospun nanofibers could be developed, as these materials can be used to disinfect sewage treatment plants. Although biobased nanofibers have promising benefits when compared to commercial filters, it is important to consider the manufacturing processes. Through this process, the electrospun nanofibers derived from natural biopolymers result in lower CO_2 emission when compared with others such as synthetic membranes, activated carbons, and carbon nanotubes (Paradis-Tanguay *et al*. 2018). Moreover, the world's ground and surface water are heavily contaminated and unsafe for human consumption. Therefore, water contamination will also become a major concern and focus for most wealthy countries as regulations become more rigorous (Ali *et al*. 2012). Pharmaceutical active compounds (PhACs) have been listed as the main issue in water quality research, and up to 90% of PhACs supplies are excreted as unmetabolized products in urine or stools, where they enter household wastewater systems. These products are discharged into the atmosphere as parent chemicals or active metabolites via effluents from WWTPs due to poor water treatment. However, many countries have shown concern about the presence of pharmaceutical residues in the marine ecosystem due to their potential for negative effects on the natural environment and human health (Ebele *et al*. 2017b).

Thus, appropriate treatment procedures for pharmaceutical wastewater should be established and deployed in response to the growing demand for wastewater remediation strategies (Patel *et al*. 2019). Such post-treatment procedures as ozonation, membrane filtration (MF), and adsorption onto activated carbon (AC) can remove the majority of PPCPs contaminants (Oulton *et al*. 2010). However, there are some disadvantages, as therapeutic methods such as ozonation is either too expensive; it was inappropriate due to high production and maintenance expenses, as well as the fact that it was found to be unfriendly to the environment (OECD 2019). Recently, novel membrane technologies have attracted interest in cleaning wastewater of pathogens, micropollutants, and salts using membrane filtration (MF) (Kamaz *et al.* 2019). The molecular weight cut-offs of membranes allow them to be classified into four groups: microfiltration (MF), ultrafiltration (UF), nanofiltration (NF), and reverse osmosis (RO). Typically, micro- and ultrafiltration are installed as pretreatment devices in low-pressure contexts, whereas nanofiltration and reverse osmosis are typically used at high pressures to remove micropollutants. Physically, NF and RO membranes are the only membranes that would be suitable for PPCP removal purely on the basis of size exclusion mechanisms. Since activated carbon has a large micropore volume and a high surface area, it is widely used as an adsorbent in water treatment for organic and non-polar substances (Zhang et al. 2015) (Cevallos-Mendoza et al. 2022). Indeed, AC and zeolites have been investigated as some of the most widely utilized and effective adsorbent materials for wastewater treatment. Despite their high efficiency, these adsorbents generate a host of issues, including stabilization and recycling, necessitating time-consuming and expensive regeneration

methods (Kyzas *et al*. 2014a). WWTPs typically have a primary physicochemical treatment solution and a secondary system made up of activated sludge produced by a biological reactor. Simply put, these traditional treatment plants are ineffective in removing pharmaceuticals, and although they clean the wastewater, they are neither sustainable nor economical (Oulton *et al*. 2010).

Pharmaceutical products have been treated in wastewater treatment facilities (WWTPs) and are not eliminated from the environment. Such pharmaceuticals as carbamazepine, atenolol, acetylsalicylic acid, diclofenac, and 890 lincomycin have remediation efficiencies as low as 10% (Patel *et al*. 2019). In addition, pharmaceuticals cannot be entirely degraded in WWTPs since they are designed to handle organics in the mg/L range that are easily and partially degradable. However, pharmaceutical solubility, absorbability, volatility, biodegradability, polarity, and lifespan are variable and can be observed at extremely low concentrations (ng/L-g/L) (Ziylan and Ince 2011). Most of the time, first and secondary WWTP treatments are insufficient to remove these contaminants, hence, allowing them to enter the drinking water system. As a result, as the population grows and per capita, opioid consumption rises, complex and effective tertiary treatment techniques will be required. Pharmaceuticals can be separated from water and wastewater using advanced oxidation processes (AOPs) and adsorption. AOPs and other therapies, on the other hand, generate a lot of oxidation and transformation products, some of which are toxic (Patel *et al*. 2019).

Adsorption is a prominent physical approach that is used to eliminate trace organic pollutants from water, and it is one of the key methods believed to be an effective treatment and low-cost process for removing most evolving chemicals from water (Mohammed Mageed 2013). The main advantage of adsorption is that it does not produce by-products that can be more harmful than the parent molecule. Processes for eliminating PPCPs ought to be quick, simple, cost-effective, reusable, and environmentally benign (Gomes *et al*. 2017). Furthermore, unlike other approaches, adsorption does not necessitate the creation of materials. However, during usage, adsorption demands the regeneration or disposal of substantial volumes of adsorbent. Therefore, it is vital to destroy recoverable medicines and derivatives. To overcome these constraints, a significant effort has been made to develop novel, efficient, and ecologically friendly adsorbents based on low-cost and natural polymeric materials (Kyzas *et al*. 2014b).

In adsorption applications, chitosan has proven to be an effective and versatile material. As a result of previous literature in the field, researchers have modified chitosan with a variety of functional groups. By the presence of amino and hydroxyl groups in chitosan molecules, the chitosan can be modified, which can facilitate many possible adsorption interactions between modified chitosan and pollutants (dyes, metals, ions, phenols, pharmaceuticals, pesticides, herbicides, *etc*. (Kyzas and Bikiaris 2015). Additionally, these functional groups can be modified either by cross-linking or grafting to improve adsorption efficiency and specificity (Mourya and Inamdar 2008; Cheung *et al*. 2015). Because of its high abundance of amino and hydroxyl functional groups, the use of CS as an adsorbent has lately sparked the interest of researchers in the water and wastewater treatment sectors (Naghizadeh and Nabizadeh 2016). CS has a chemical composition that enables intricate polymer design alterations for specific purposes, unlike other polysaccharides (cellulose or starch). However, the primary hydroxyl and amine groups found on the backbone of CS are also responsible for the polymer's reactivity and serve as chemical modification sites. Moreover, composites made up of a variety of compounds are more capable of adsorbing and avoiding wastewater pollutants in acidic

environments (Giri *et al*. 2012). Despite the material's remarkable qualities, membranes made from it are frail and brittle, having low mechanical strength and flexibility. Cross-linked CS has been shown to have better mechanical qualities than individual CS among the ways utilized to improve CS mechanical properties (Pereira *et al*. 2019).

There are various derivatives generated from CS either by chemical or physical modification of the raw CS. In principle, chemically modified CS could result in some products or materials with qualities suited for the elimination of specific contaminants. The steps involved in CS modification include cross-linking and grafting of the CS backbone impregnation (Brasselet *et al*. 2019). Several attempts have been undertaken to change CS after graft modification in order to increase its solubility and physicochemical qualities (Shariatinia and Jalali 2018). Such chemical changes should not change the core structure of CS. However, this modification introduces new derivatives with improved features for specific applications in other domains of use.

Due to cooperation among numerous intermolecular hydrogen bonds (H-bonds), CS cannot be soluble in water. However, various modifications can be made on the -OH and -NH_2 positions to improve its water solubility (Santos Miranda *et al.* 2006). Accordingly, the amino group of CS was derivatized by a succinyl group in this study. Specifically, it was modified through N-acylation with succinic anhydride. By adding the -COOH function through the succinyl group, hydrophilicity is improved (Mura *et al.* 2011; Bashir *et al.* 2016). By forming electrostatic and hydrophobic interactions with the target molecular, hydrophilicity also improves its attractive properties. Since NSCS has weaker hydrogen bonding interactions than CS, its water solubility has been dramatically improved (Mourya and Inamdar 2008; Lu *et al.* 2009). A succinylation reaction occurs when the polysaccharide amine group condenses with the anhydride's electrophilic carbonyl group, followed by the formation of an amidic bond with the anhydride ring. The primary amine from the glucosamine component of CS attacks the carbonyl carbon of succinic anhydride in a nucleophilic manner. As oxygen from hydroxyl groups has a nucleophilic character, the O-substituted derivative can be formed. Although oxygen electrons are much more readily available than nitrogen electrons, the N-substituted derivative is preferred (Bashir *et al.* 2017). The chemical structure of NSCS, which has strong water-solubility, is shown in Scheme 1 (Tan *et al.* 2009; Zhou and Wang 2009). NSCS was precipitated after the reaction in the form of a salt ($RCOO^- Na^+$) with a greater water interaction as a result of a change in pH. Succinyl groups were transplanted onto CS to provide a hydrophilic group, but not all intermediate products (NSCS) were water-soluble.

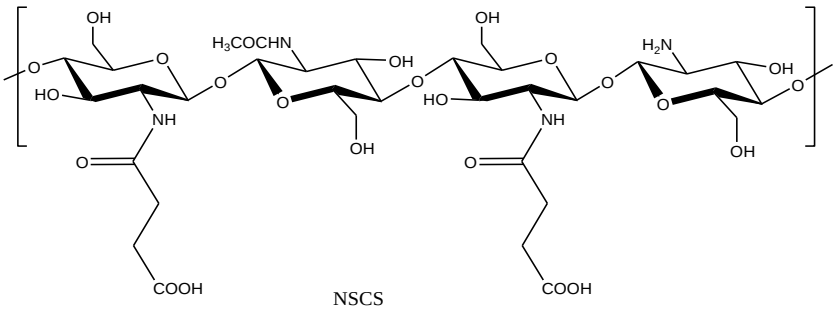

Scheme 1. The chemical structure of N-succinyl chitosan

As a result of this approach, the adsorption properties of CS are strengthened, as well as the mechanical intensity and chemical stability of CS in acidic conditions (Guibal 2004; Vakili *et al*. 2014; Naghizadeh and Nabizadeh 2016). Various approaches such as chemical and physical modification of CS, which depends on its application, could be maximized to modulate the polymer reactivity and boost the adsorption kinetics (Vakili *et al*. 2014). In addition to boosting biodegradability and antibacterial activity, the hydrophilicity generated by the introduction of polar groups capable of forming secondary contacts is a benefit of altering CS. In achieving an appropriate mechanical strength as an artificial medical device, dispersion of growth factors, and degradability are considered important obstacles for potential alteration procedures (Chen and Liu 2016). Furthermore, benefits of CS over the conventional AC and other bio-sorbents can include low prices, a high tolerance for some toxins (because of the addition of amino and hydroxyl groups), chemical stability, high reactivity, and emission selectivity. N-succinyl chitosan (NSCS) is created by adding succinyl groups to the N-terminal of chitosan's glucosamine units. Previous studies revealed that NSCS has improved biological and physicochemical qualities, and therefore, the market price of NSCS may rise (Zhou *et al*. 2018). This is due to its appealing and inherent features, such as facile solubility in a variety of pH levels without the need for an acidified media, high hydrophilicity, and biocompatibility, which all present in pristine CS (Kamoun 2016). To allow better interaction with water molecules, succinyl groups were added to the N-position of the glucosamine units of CS, which is a favourable material because of its solubility, biodegradability, and low toxic (Kato *et al.* 2001; Sun *et al*. 2013), and biocompatibility (Bashir *et al*. 2017; Lucas de Lima *et al*. 2020). Many functional groups such as amine and hydroxyl could be found in the CS chain and despite its widespread application, the adsorption capacity of CS has yet to be fully realized (Sun *et al*. 2013), and no previous research on the adsorption capabilities of NSCS/PEO nanofiber has been published. Many reactive functional groups, amino groups, carboxyl groups, and both primary and secondary hydroxyl groups at the C-3 and C-6 positions, respectively, are present in NSCS, a well-known CS derivative (Sun *et al*. 2013) Therefore, since NSCS is made up of -NH and -COOH groups, and it can easily react with a wide range of agents (Bashir *et al*. 2017).

To compete with AC and obtain a satisfactory adsorption capacity for trace pharmaceutical pollutants, the surface area of material must be increased (Patients *et al*. 2012). One of the strategies to achieve this step is electrospinning. Electrospinning is a straightforward method for creating nanofibrous substrates with variable fibre sizes (Patients *et al*. 2012). Electrospun nanofibers have attracted a lot of attention because of their unusual properties, which include a large surface area, low weight, nanoporous features, and design flexibility for specific physical and chemical functionalization. However, because the entanglements and overlaps between polymer chains play a critical role in manufacturing bead-free and uniform nanofibers, high molecular weight polymers and high solution concentrations are commonly used in electrospinning. It has been shown that electrospinning low-molecular-weight compounds is a difficult task to achieve (Celebioglu and Uyar 2013). The relevance of elasticity and relaxation time rather than molecular entanglements for electro-spinnability of solutions has also been established. Interestingly, over 30 polymers have been electrospun successfully so far (Duan *et al*. 2004), but no published work on the electrospinning of NSCS/PEO has been discovered by authors. Herein, we are reporting for the first time the use of electrospinning fibres using electrospinning blended NSCS/PEO solutions in aqueous acetic acid.

This superstructure of NSCS/PEO nanofiber with many reactive functional groups may allow for robust attachment to pharmaceutical contaminants in wastewater and improving adsorption capacity level. The possibility of developing a novel NSCS including nanofibers by electrospinning from NSCS/PEO mix solutions was demonstrated in this study. According to the authors' first published paper, high adsorption capacities were achieved after electrostatic interactions between N,O-carboxymethyl chitosan/PEO nanofibers and fluoxetine (FLX). The present study extends the research to modify the chitosan by increasing its hydrocarbon content to determine if this would affect FLX's adsorption capacity. To test whether hydrophobic groups will enhance the adsorption capacity of modified chitosan, it is necessary to increase the hydrocarbon surface area so that hydrophobic interaction will be included in addition to electromagnetic interaction.

To our knowledge, there has been no research into the application of using modified NSCS/PEO nanofibers mats to remove the pharmaceutical residues (antidepressant fluoxetine) from wastewater. The effect of the pH of FLX solutions, the contact temperature, the adsorption mechanism, and the contact time of single and various pharmaceuticals contaminate on the NSCS/PEO were studied. The adsorption capability of FLX and VEN (antidepressants), CBZ (anticonvulsant), and IUP (anti-inflammatory) on produced nanofibers from aqueous solutions were investigated. The tests were carried out in batch systems. Equilibrium condition were used to determine optimum adsorption conditions for NSCS/PEO to adsorb FLX. Adsorption kinetic tests were performed. Furthermore, desorption tests with various eluents were also conducted to assure the nanofibrous membrane's reusability and to quantify their possible environmental impact.

EXPERIMENTAL

Materials

Low molecular weight chitosan (CS MW 50,000 to 190,000 g/mol, 75 to 85% deacetylated) was from Sigma-Aldrich (Reykjavik, Iceland). Polyethylene oxide (PEO) that was used as a co-spinning agent had a molecular weight of average of 900,000 g/mol was from Sigma-Aldrich (St. Louis, MO, USA). Succinic anhydride from Sigma-Aldrich (CAS 108-30-5), sodium hydroxide (NaOH), dimethyl sulfoxide DMSO, acetone, and ethanol were of analytical grade. As a model contaminant, the acquisition of fluoxetine hydrochloride (FLX) (CAS 56296-78-7), venlafaxine hydrochloride (VEN) (CAS 99300-78-4), carbamazepine (CAB) (CAS 298-46-4), and ibuprofen (IBU) (CAS 15687-27-1) were provided by Sigma-Aldrich (Oakville, ON, Canada) for the adsorption test. Methanol (HPLC grade), acetonitrile (HPLC grade), O-phosphoric acid (HPLC grade; 85 wt./wt. %), and glacial acetic acid ACS reagent (99.7 %) were purchased from Fisher Scientific (Ottawa, Ontario, Canada). The water for the experiments was prepared with a reverse osmosis membrane, Siemens Super Transparent RO, to achieve 0.055 μS /cm conductivity. Deionized water was used for testing throughout all the studies (Siemens Ultra Clear RO).

Synthesis of N-Succinyl Chitosan (NSCS) Polymer

Ring-opening reactions with succinic anhydride in a dimethyl sulfoxide (DMSO) framework yielded NSCS. NSCS was synthesized in the manner previously described (Zhou and Wang 2009; Niu *et al*. 2020). First, 2 g of CS powder was applied to 40 mL DMSO and thoroughly mixed. Second, succinic anhydride (4 g) was slowly applied to the CS solution and allowed to react for 6 h at 65 °C.

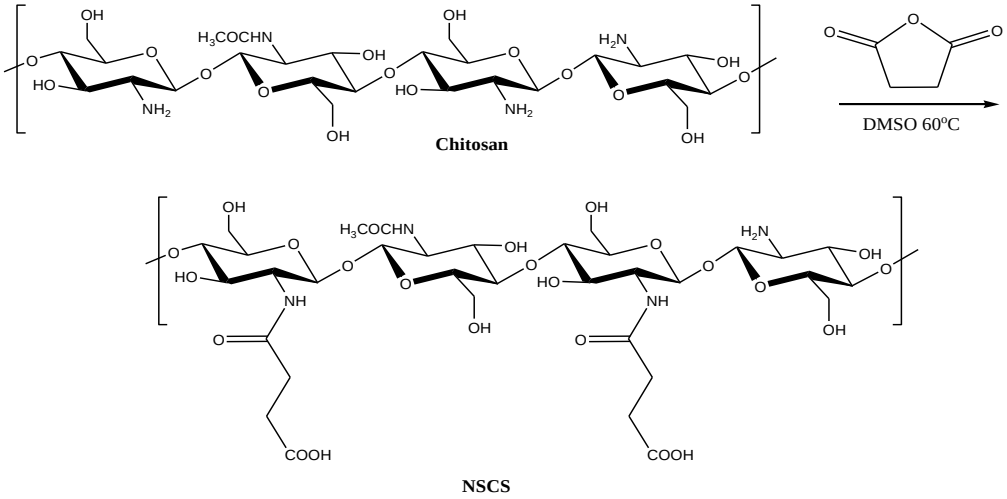

Scheme 2. Preparation of N-succinyl chitosan

The sample was dissolved in ethanol at room temperature and reacted for 1 h after being filtered to eliminate the solvent. The pH of solution was changed from 10 to 12 with NaOH (1 M) at the end of the reaction. The precipitate was dissolved in 90 mL of distilled water, then 270 mL acetone was added, accompanied by washing and precipitation with ethanol and acetone, respectively, after the mixture was filtered. Ultimately, NSCS was dried in a vacuum oven at 50 °C. Scheme 2 shows the NSCS synthesis.

Characterization of N-succinyl Chitosan (NSCS)

Fourier transform infrared (FTIR) was utilized to examine and identify functional groups on CS and NSCS. At room temperature, the FT-IR spectrum of CS and NSCS was recorded using an FT-IR spectrometer (Nicolet iS10, Thermo Scientific). The specimen was scanned from 600 to 4000 cm^{-1}. The ^{1}H-NMR spectra were calculated using a (200 MHz Oxford NMR spectrometer) with CS dissolved in D_2O as solvent and NSCS dissolved in D_2O/DH_3COOH as solvent, with chemical shifts provided in ppm. Furthermore, the degree of succinylation in D_2O/CH_3COOH was determined using the potentiometric titration method, as well as ^{1}H-NMR.

Determination of degree of substitution (DS) of N-succinyl chitosan (NSCS)

The degree of substitutions (DS) of NSCS samples was calculated using a potentiometric titration method (Sun and Wang 2006a; Wang and Wang 2008). Briefly, dried NSCS (0.20 g) was dissolved in 0.1 mol/L hydrochloric acid solution (20 mL). Methyl orange was used as an indicator for the endpoint determination. A standard 0.1 mol/L sodium hydroxide solution was used during titration (Lu *et al*. 2004; Sun and Wang 2006a). The cumulative DS of NSCS samples was determined using Eqs. 1 and 2,

$$DS = \frac{161A}{M_{NSCS}} - 58A \quad (1)$$

$$A = V_{NaOH} \,.\, C_{NaOH} \quad (2)$$

where M_{NSCS} is the mass of NSCS (g), V_{NaOH} and C_{NaOH} represent, respectively, the volume and molar concentration (M) of NaOH, and finally 161 and 58 are associated to the molecular weights of the chitosan (glucosamine) and the SCS group.

Zeta potential (ZP) measurement

The zeta potential (ZP) of NSCS was measured at room temperature (23°C). The zeta potential can be defined as the electrical potential at a hydrodynamic slip plane adjacent to the NSCS. To calculate the ZP, a 1 M (10 mL) solution of NSCS was dissolved in distilled water for 1 h with gentle shaking at room temperature, and the pH values ranged from 2.0 to 11. NaOH (0.01 M) was used to neutralize the pH of solution. The ZP in solution was determined using a Zetasizer Nano (Malvern Instruments Ltd., model ZEN 3600).

Preparation of Solutions and Operating Procedures for Electrospinning of NSCS/PEO Nanofibers

The electrospinning unit was set up as shown in Fig. 1. NSCS (8 wt%) and PEO (5 wt%) solutions were prepared separately by dissolving in 50% acetic acid (AA) at room temperature (23 °C) until a homogeneous viscous solution was obtained (1 h, NSCS; 20 h PEO) after agitation at 200 rpm. The mass ratio of NSCS/PEO was set to (3:2, 5:5 and 6:4 m/m), and the resulting solution was stirred for 2 h at 200 rpm. To remove bubbles, the mixture was placed in an ultrasonic bath for 15 min. Finally, the mixture was allowed to rest for 3 h before being used in the electrospinning process. The electrospinning fluid (NSCS/PEO) was pushed into a 5 mL syringe with a 20-gauge needle and attached to a syringe pump device (KD Science, model 100) that provides a steady and slow liquid flow. For the electrospinning phase, the flow rate was 0.2 to 0.5 ML / h. The distance between the nozzle tip and the collector was measured with a syringe pump positioned at a horizontal gap (10 to 15 cm). Throughout the electrospinning, the height of the syringe pump was kept constant. During the electrospinning process, a metallic wireframe was used as a collector, and the needle and collector were both connected to a power supply (Gamma High-Voltage Research USA) that produced a high-voltage output. The voltage ranged from 7 to 14 kV. Different electrospinning conditions were tried for each NSCS/PEO ratio by changing the flow rate, current, and distance between the needle and collector (wireframe) to obtain the optimal jet (steady jet with limited drop projections) and narrow beadle nanofibers. Both experiments were carried out at room temperature (23 °C) in a handcrafted electrospinning enclosure. Between the two layers, relative moisture was preserved (30 to 40%). The nanofibrous mat was removed from the frame at the end of the electrospinning process and dried in an oven (Fisher Scientific Isotemp Oven, Thermo Scientific HERATherm Oven) at 80 °C for 24 h.

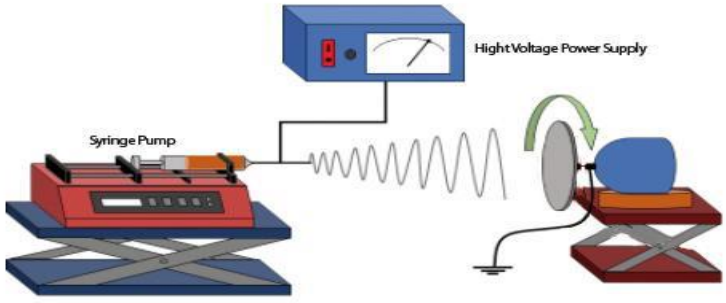

Fig. 1. Schematic representation of electrospinning setup

Nanofibers Characterization

The morphology of the nanofiber membrane was assessed before and after the adsorption test using an SEM (A Hitachi SU1510 Scanning Electron Microscope). This was used to image the morphologies and diameters of nanofibers. Furthermore, the diameter was calculated using Image J tools (Rasband, W. S., ImageJ, US National Institutes of Health, Bethesda, MD, USA, https://imagej.nih.gov/ij/,1997-2018). The diameter of 50 nanofibers obtained on 3 different photos (a total of 150 nanofibers per sample) was measured in order to achieve an average value. And the data are presented as the average ± standard error.

Batch Adsorption Procedure

A stock solution of FLX was prepared using deionized water. The pH of solutions was adjusted as needed with HCl (0.01 M) or NaOH (0.01 M). By employing a pH meter, the initial pH (natural pH solution of FLX 5.5) value was 5.5 during the batch experiments so pH adjustment was made throughout the study to reach pH values of 3 to 10. Therefore, the effects of pH FLX on Q_t values at room temperature (RT) for varying contact duration were investigated in this study. Individual (FLX) and multiple pharmaceutical contaminants (FLX, IBU, VEN, and CAR) batch adsorption on NSCS/PEO membranes was investigated. By dissolving the corresponding stock solutions in a 5% methanol solution, separate 2500 ppm standard solutions of FLX, VEN, CAR, and IBU were prepared. These solutions were then diluted in preparation for adsorption tests. Stock solutions (2500 ppm) of FLX, IBU, VEN, and CAR were made by weighing and dissolving the required amount of the corresponding substance in 5% methanol. The homogeneity of the solution, as well as the temperature and pH of the medium, were all checked ahead of the start of the sorption tests. A 50 ppm FLX solution was used as a model of contaminated water in tests using one contaminant on NSCS/PEO membranes. For tests with multiple contaminants, 12.5 ppm of FLX, IBU, VEN, and CAR were added to simulate contaminant water. The tests were carried out over a 150 min period to ensure that equilibrium was reached. Sorption tests were carried out with a 25 mg sample of the membrane inserted into conical flasks (250 mL) containing 50 mL of an FLX solution as a single contaminant model (50 ppm) and 5% of methanol. The agitation speed was adjusted at 200 rpm for all adsorption-desorption tests using (ORBIT Environ-shaker, Lab-Line) under controlled temperature. Before insertion of the membrane into the solution, an aliquot of 500 µL was sampled to determine the initial FLX concentration. Batch tests were conducted over 150 min to ensure that equilibrium was achieved prior to the collection of a 500 µL aliquot. The adsorption capacity at time t (Q_e) was determined using Eq. 3,

$$Q_e = (C_\circ - C_e)\ V / W \quad (3)$$

where C_e is the final concentration of contaminant (ppm) at time t (min), C_o is the initial concentration of contaminants (ppm), V is the volume of solution (L), and W is the mass of adsorbents (g).

In order to determine the residual concentration of FLX in water samples during our batch adsorption tests, a high-performance liquid chromatography (HPLC) system (Shimadzu Prominence I - series) coupled with a diode array detector (DAD) was used. The chromatographic separation was achieved using a C18 reverse-phase column (XB-C18, 100 Å, 150 x 3 mm, 2.6 µm particle size, Phenomenex, Kinetex®). The residual concentration of FLX in an aqueous solution was determined by HPLC-UV DAD, using a strategy devised by Camiré *et al*. (2020a).

Kinetic Test

Pipetting (500 µL) samples at room temperature with an initial concentration of (50 ppm) of FLX yielded kinetic curves, and the concentration of FLX was measured by HPLC-UV DAD. During the adsorption, such determinations were carried out at brief intervals until equilibrium was attained. Samples of FLX solution were taken at 5, 10, 15, 20, 30, 40, 50, 60, 75, 90, 120, and 150 min after the adsorbent was added. To determine the equilibrium time at 150 min, a kinetic adsorption test was done first. The injected samples' adsorption capacities were calculated, and a curve showing adsorption capacity over time was created. The tests were repeated in triplicate, and a mean curve was calculated. To examine kinetics adsorption data, the pseudo-first-order and pseudo-second-order rate equations are commonly used (Min *et al*. 2016). Adsorption can be characterized using a variety of adsorption kinetics models. For characterizing the adsorption mechanism in this study, pseudo-first-order (PFO) and pseudo-second-order (PSO) kinetic models were utilized. Nonlinear pseudo-first-order (Eq. 4) and nonlinear pseudo-second-order (Eq. 5) models were used to fit experimental data (Hamdaoui 2006),

$$Q_{\mathrm{t}} = Q_{\mathrm{e}}\left(1 - \exp^{-k_1 t}\right) \quad (4)$$

$$Q_{\mathrm{t}} = \frac{k_2 Q_{\mathrm{e}}^2 t}{1 + k_2 Q_{\mathrm{e}} t} \quad (5)$$

where Q_e, is the amount adsorbed (mg/g) at equilibrium; Q_t, is the amount adsorbed (mg/g) at time t (min); k_1 is the pseudo-first order (PFO) adsorption rate constant (g/g min^{-1}); and k_2 is the pseudo second order (PSO) adsorption rate constant (g/g min^{-1}).

The kinetic parameters (maximum adsorption capacity and kinetic constant) for all models were determined using the kinetic equation, the solution function in Microsoft Excel, nonlinear regression analysis, and MATLAB software. The obtained parameters were used to plot pseudo-first order and pseudo-second-order curves, which were then compared to experimental data.

The adsorption kinetics data were fitted using different models in order to gain a better understanding of the mechanism of NSCS/PEO membrane adsorption. The pseudo-first-order and pseudo-second-order rate equations were used (Hamdaoui 2006).

Desorption Experimental

Desorption is the reversal of adsorption, and it is particularly important since it determines the adsorbent's capacity to be reused (Gabelman 2017). The NSCS/PEO mats were rinsed with deionized water after adsorption and dried overnight at room temperature. At low pH, desorption studies on the recyclability of the NSCS/PEO nanofibers were done utilizing several circumstances, including a 1M HCl and 5% acetic acid solution. In addition, heating of the solution in an ultrasound bath (sonication) by using hot water was used to realize the effect of temperature and sonication on the adsorption and desorption of FLX. Methanolic solutions (100%) were used to assess the environment in which the contaminant is strongly soluble. In all cases, the membranes were soaked in a solution (50 mL) for 3 h. To assess the recovered FLX concentration, original and final tests were loaded into HPLC-UV DAD. For numerous adsorption/desorption cycles, the desorption technique with the best desorption performance was chosen to assess reusability. Between each measurement, the membranes were removed and dried in a vacuum desiccator.

RESULTS AND DISCUSSION

Structural Characterization of N-Succinyl Chitosan (NSCS)

Based on IR and ^{1}H-NMR spectroscopy, the succinyl groups were grafted onto the amine group of CS in this study (Bashir *et al.* 2017). Since succinylation occurs predominantly at the N-position of CS, the number of amino groups, which serve as the key adsorption sites in CS, decreases as N-succinylation increases, resulting in a decrease in adsorption. In contrast, the adsorption potential of NSCS increases marginally with increasing DS (Sun and Wang 2006b). A previous study by Skorik *et al.* (2017) suggests that homogeneous and heterogeneous conditions are crucial synthesis parameters that can affect the reaction between CS and succinic anhydride that impacts the DS of NSCS.

Figure 2 shows the FT-IR spectra of CS and NSCS. The most compelling evidence of the successful transformation of CS to NSCS came from the transformation of the amine (NH_2) absorbance observed in the spectra of CS at 3358 cm $^{-1}$. The disappearance of this absorbance coupled with the appearance of a carbonyl peak representing the new amide functionalities at 1648 cm^{-1} demonstrated that the amide (-NHC=O) had been formed. Further evidence for the generation of NSCS came from the (-NH) absorbance peak at 1559 cm^{-1} and a new peak appeared at 1728 cm^{-1}, which was assigned to (-COOH) which is characteristic of NSCS (Lu *et al*. 2009; Li *et al*. 2019; Zhang *et al*. 2014).

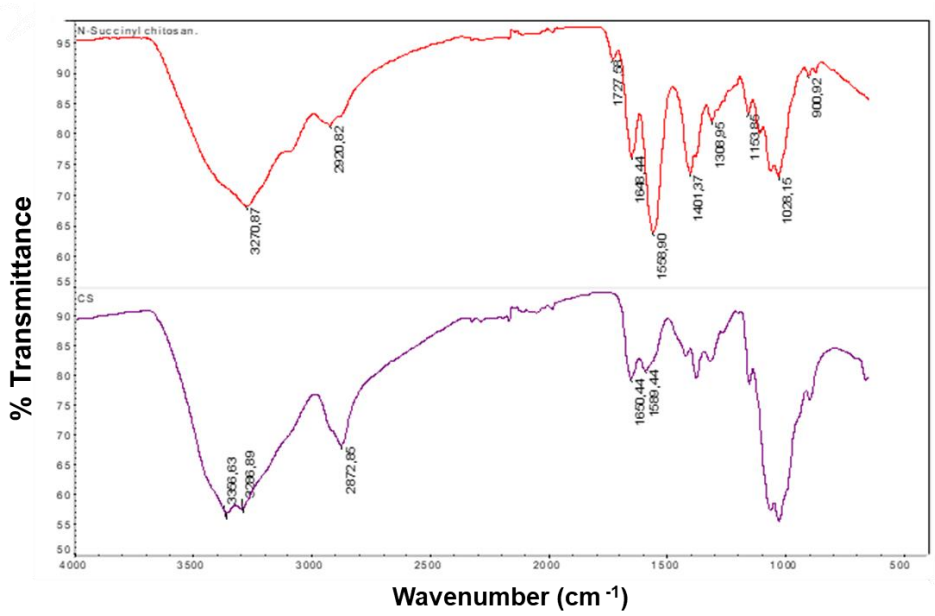

Fig. 2. FTIR spectra of CS and NSCS

The ^{1}H-NMR results further supported the transformation of CS to NSCS. A triplet observed at 1.0 ppm in the spectrum of NSCS is characteristic of the CH_2CH_2 moiety belonging to the succinyl group ($NHCOCH_2CH_2COOH$). Peaks at 3.4 to 3.6 ppm are characteristic of CS and belong to the CS backbone hydrogen (Bashir *et al*. 2017). As such, these peaks are present in the ^{1}H of both CS and NSCS, as shown in Fig. 3. Similar observations are reported in literature (Lu *et al*. 2009; Zhang *et al*. 2014).

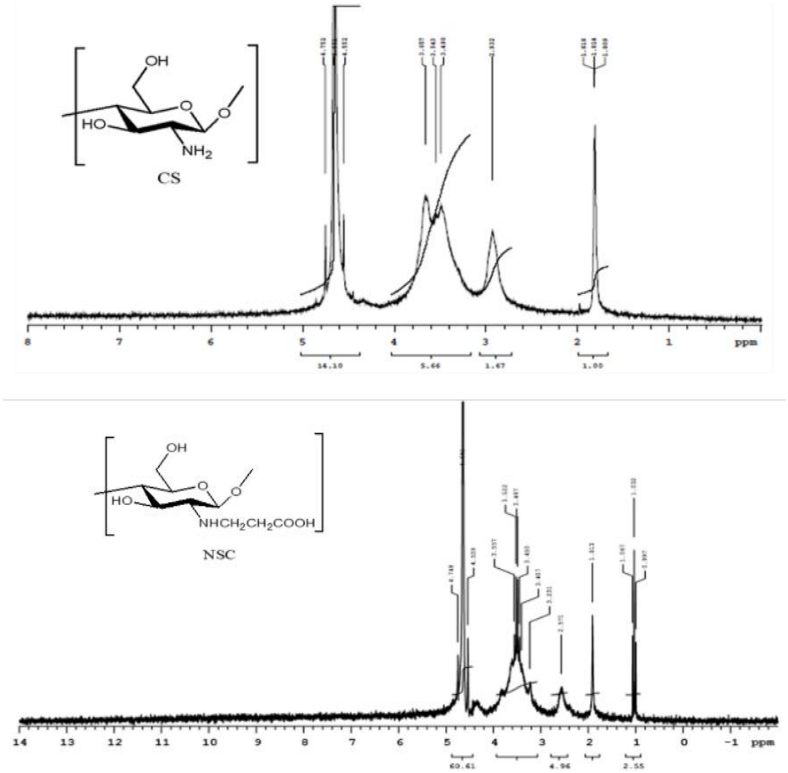

Fig. 3. ^{1}H NMR spectrum of CS in D_2O and NSCS in D_2O / CH_3COOH

Measurement of Zeta-Potential (ZP) and Potentiometric Titration

Surface charge is a primary parameter determining the grafted carboxylic acid moieties on the surface of the modified polymer, which leads to probable electrostatic interactions between NSCS and FLX molecules. Figure 4 depicts the modified polymer's ZP at various pH levels. A potentiometric titration method and ^{1}H-NMR in D_2O/CH_3COOH revealed a succinylation degree of 35%. The pH-dependent ZP of NSCS ranged from + 26 mV at pH 3.0 to - 41.5 mV at pH 10.0. As shown in Fig. 4, the isoelectric pH (pH_{iep} = 6.3), and the ZP NSCS had a positive value at acidic pH that rose from 15 to 26 mV as the pH was decreased. At basic pH, the ZP decreased to negative values as the pH rose. This indicates that NSCS became highly ionized with negative charges due to larger amount of deprotonated carboxyl groups (-COO^{-}). These findings are in agreement with published studies (Miranda *et al*. 2006; Monsalve *et al*. 2015).

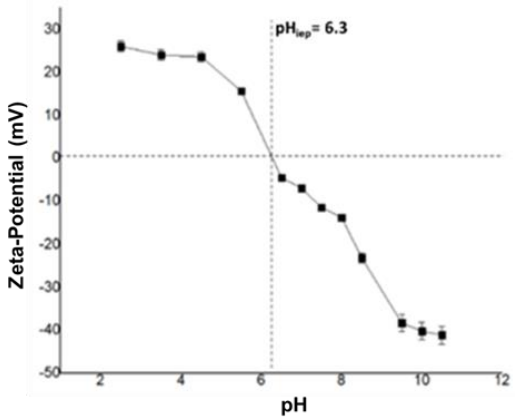

Fig. 4. Zeta potential of NSCS as a function of pH

Characterization of NSCS/PEO Nanofibers

Electrospinning is a flexible and effective nanofiber-making process. Beads were present in large amounts in the electrospun materials used in this study. The primary cause of beads was relatively low values of surface tension. As the surface tension of electrospun materials increases, the size and number of beads decreases (Miranda *et al*. 2006). Electrospinning parameters, which are important to comprehend, affect the diameter and morphologies of electrospun fibres. To achieve the desired fibre morphologies and diameters, these parameters can be easily adjusted. The three main categories that affect electrospun fibre parameters such as morphology and diameter are (a) intrinsic properties of the solution, (b) manufacturing conditions, and (c) atmospheric parameters (Williams *et al.* 2018). Electrospun NSCS/PEO nanofibers with the smallest diameters were around (183 ± 38 nm). Even though the fibre diameters were high in comparison to the diameter of pure CS/PEO ratio 4:1 (140 ± 53 nm) as reported in our previous work (Khierallah *et al*. 2021), the solvent evaporation rate during electrospinning was slow. A 50% acetic acid solution, which is easier to evaporate than water, was tried as a solvent, but the efforts were not successful in controlling other defects such as the droplet production, unstable jet, formation of particles-nanofiber, and very large diameter nanofibers. In addition, it resulted in low adsorption capacity for FLX. One basic parameter, such as NSCS solution concentration/viscosity, was used to monitor fibre diameter, with increased viscosity resulting in thicker fibres. The concentration of polymer solution has a huge impact on electrospun nanofiber formation. The viscosity of a solution is considered to be proportional to the viscosity of a polymer solution (Angammana and Jayaram 2016). The greater the nanofiber diameter, the higher the viscosity of sample. As a result, fibre production in electrospinning requires a minimum concentration. This was the most difficult part during electrospinning, so different conditions were employed in an effort to form the continue nanofiber with small diameters. Furthermore, electrospray forms in its position when very low amounts of electricity are electrospun. This is due to the solution's high surface tensions and low viscosity.

The concentration and mass ratio NSCS/PEO of the solution are two of the most important parameters affecting the electrospinning process, and they play a crucial role in creating defect-free nanofiber mats, as shown in (Fig. 5A). The copolymer, on the other hand, was the most important factor influencing the electrospinning operation. As a result, increasing the amount of PEO (Co-polymer) in the solution aided in the manufacture of the best NSCS/PEO nanofiber (6:4 mass ratio). Moreover, when the viscosity was low, and the distance between the needle and the collector was longer, a higher voltage was needed. In fact, CS solutions containing 100% was not tested. Attempts were made to compare the three mass ratios (2:1, 3:2, and 6:4) when the NSCS concentration was increased from 3% to 8%, respectively, in this analysis. In order to find the optimum electrospinning parameters and the highest adsorption potential, the viscosity of the solutions was increased by increasing the concentration of the solution. The following parameters were optimized: a distance of 10 to 15 cm between the needle and the collector was configured, with a flow rate of 0.01 to 0.5 mL/h. The optimum voltage, which ranged from 7 to 14 kV, was calculated by observing the jet behaviour. The three sets of parameters were 2:1 (0.01 mL/h, 8kV, 15 cm), 3:2 (0.3 mL/h, 12 kV, 12 cm), and 6:4 (0.5 mL/h, 14 kV, 10 cm). Despite this, due to its low viscosity, a pure NSCS aqueous solution is not electrospinnable. As a result, PEO is often applied to the NSCS solution to improve its electrospinnability. The hydrogen-bonding interactions between the hydroxyl groups of PEO and NSCS make them completely compatible and miscible. NSCS has a lower viscosity than pure CS. Since

mild viscosity is needed for electrospinning processes, raising the voltage beyond a certain point resulted in much more liquid droplet projection on the collector surface, as well as destabilization of the jet. To solve this problem, the concentration of the solution was increased while carefully lowering the flow rates and distance.

Due to the larger surface area in the corners of the frame during an electrospinning operation, a nanofiber web begins to form, resulting in the build-up of surface charges (Kyzas *et al*. 2016; Ilse *et al* 2020). As a "spider's web," the deposition process will begin until a mesh fully covers the space inside the frame. Furthermore, using a frame as a collector allowed for easier nanofiber removal, allowing researchers to quickly determine whether an electrospraying /electrospinning process is taking place. This is because even if some nanofibers are deposited, the particles will split them, preventing, or reducing mat formation. As a result, using a frame as a collector device has many advantages over using regular aluminum foil in an electrospinning setup. Reusability, a smoother mat recovery method using a simple cutter, and a quicker way to assess the morphology of the collected material are the most significant benefits (Angammana and Jayaram 2016). Scanning electron microscope (SEM) images of uniform nanofibers, particles, and beaded electrospun NSCS/PEO nanofibers prepared in the research lab are shown in Table 1. The corresponding graphs show the effects of different electrospinning parameters. The concentration and mass ratios were compared in this table. It was discovered that, even with low viscosity, most parameters created nanofibers with particles or beads, and that most electrospinning parameters produced liquid droplets in the collector's field. Nanofibers were obtained with a lot of particles and beads at low concentrations. Since the electrospinning method was quicker, simpler, and free of particles and beads than the others, the solution with an NSCS: PEO (ratio 6:4) with 8wt.%/5wt.% concentration was the best solution for processes. It also resulted in FLX having a higher adsorption capacity.

Table 1. SEM Images of NSCS/PEO Nanofiber Membranes with Different Condition Adjustments of the Electrospinning Parameters

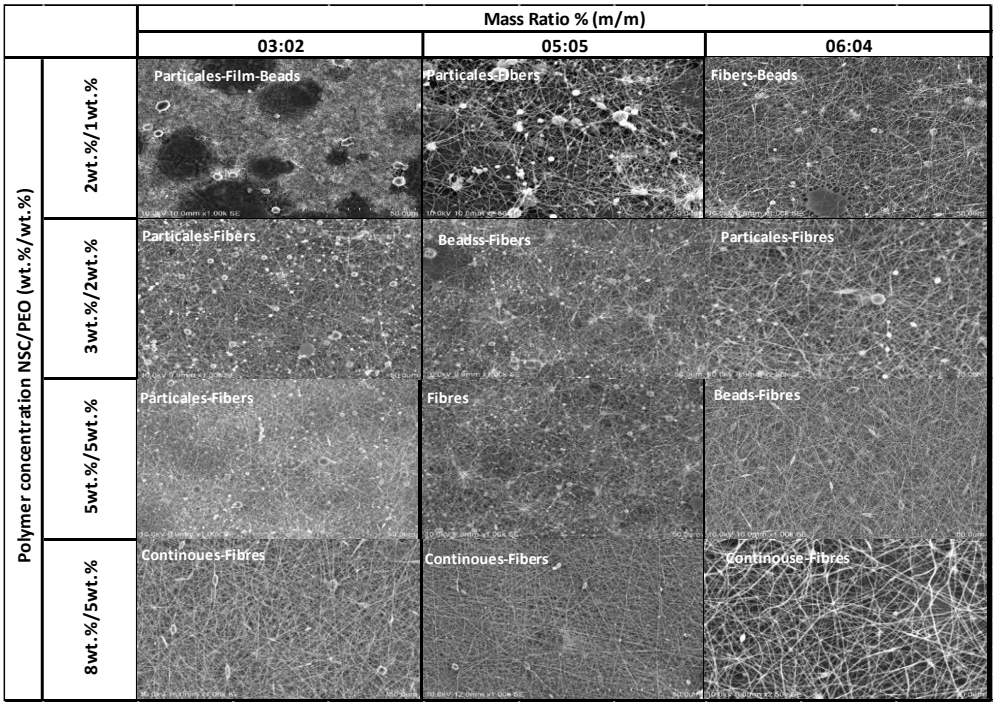

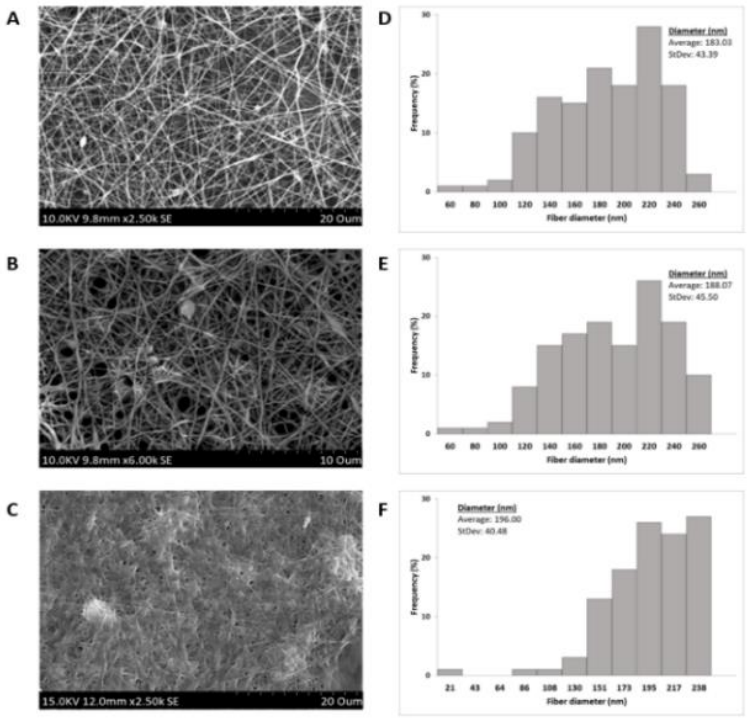

Fig. 5. SEM images of NSCS/PEO electrospun nanofibers and diameter at the concentration (8 wt%/5 wt%) (6:4 mass ratio) (A); After heat treatment of nanofibers membrane (100-150 °C) (B); after Chemical stabilization in 2% dilute acetic acid (C)

NSCS/PEO nanofiber membranes were treated with heat treatment temperatures at 100 to 150 °C (Fig. 5B) and chemical methods with 2% dilute acetic acid (Fig. 5C). It was discovered that chemical stabilization with 2 % dilute acetic acid at pH below 4.4 resulted in low weight losses of the nanofiber membranes compared to using 0.01 HCl. The diameters of nanofiber mats treated chemically with dilute acetic acid, on the other hand, were smaller than those treated chemically with HCl. Therefore, the diameter of the nanofibers were changed by stabilization test. The diameter of the nanofiber before the stabilization test was (183 ± 38 nm), and then it increased on each stabilization process. So at heat- treatment it was (188 ± 45 nm), and in chemical treatment with acetic acid it was (196 ± 40 nm), as shown in Figs. 5 (D), (E), and (F), respectively. Ultimately, due to high moisture content, efforts were not successful to electrospin NSCS / PEO under the same conditions of parameters.

Adsorption Kinetic Studies

The experimental adsorption results clearly show that FLX was adsorbed by NSCS / PEO, with an agreement that this biomaterial can adsorb FLX up to 80%. Given that adsorption is preferred at pH 8, kinetic and equilibrium studies were carried out at various pH values with additional adjustments. As previously stated, FLX adsorption on NSCS/PEO nanofibers is preferred at high pH levels. The pH of the solution has a significant impact on both the medicinal charge and the functional groups present on the NSCS surface. These findings indicate that the appropriate adsorption of FLX into NSCS/PEO transformed this inexpensive and ecologically acceptable material into a tool with promising applications in the removal of pharmaceuticals from wastewater.

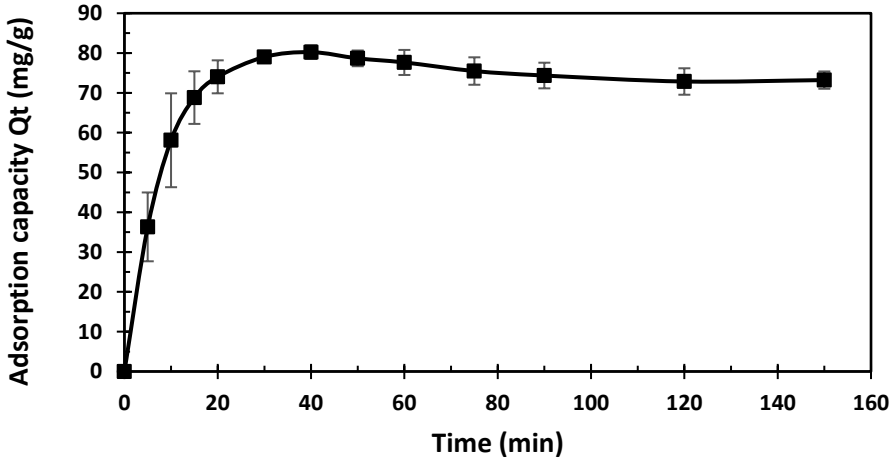

Fig. 6. Sorption capacity of FLX on NSCS/PEO nanofibers 8 wt%/5 wt% (6:4) at (pH =8).

The potential for FLX adsorption on NSCS/PEO nanofibers mass ratio (6:4) improved significantly as the adsorption time increased. In about 30 min, the maximum FLX adsorption on NSCS nanofibers was observed. Due to that, a 30-min adsorption cycle was selected to ensure that equilibrium was reached under the test conditions. Pseudo-first-order and pseudo-second-order kinetic models were used to examine the potential rate-controlling steps involved in the adsorption of FLX onto NSCS/PEO nanofibers in order to match the experimental results. Figure 9 shows the curves for the kinetic models. The experimental data map was used to measure the rate constants k_1 and k_2. Table 2 displays the kinetic models' rate constants, coefficients of correlation, and calculated Q_e values. The coefficients of determination (R^2) for pseudo-first order and pseudo-second order at pH 7.0 were (0.9908 to 0.9613), at pH 8.0 were (0.9979 to 0.9969), and at pH 9.0 were (0.9971 to 0.9713), respectively. The surface of the modified CS after FLX adsorption indicated that FLX was adsorbed effectively onto NSCS/PEO nanofibers. The findings also revealed that the adsorption of FLX was dependent on hydrogen-bond and hydrophobic interactions, as well as a mild electrostatic interaction between opposite charges (Tapdigov 2021).

Table 2. Kinetic Parameter Values in the Pseudo-first, and Pseudo-second-order Models for the Adsorption of FLX on NSCS/PEO 8 wt%/5 wt% (6:4) Nanofibers: (Original concentration 50 mg/L, pH (7.0, 8.0, and 9.0), adsorbent 25 mg, t = 150 min at RT)

Experimental	Pseudo-first-order model			Pseudo-second-order model		
pH	k_1(min $^{-1}$)	Q_e(mg/g)	R^2	K_2 (min $^{-1}$)	Q_e(mg/g)	R^2
pH 7.0	0.06424	64.79	0.9908	0.00106	74.51	0.9613
pH 8.0	0.06764	66.29	0.9979	0.001013	81.16	0.9769
PH 9.0	0.07205	71.89	0.9971	0.001178	78.75	0.9713

The mechanism of FLX adsorption onto NSCS/PEO is likely to involve electrostatic interactions, hydrophobic interaction, and the H-bond. All of these factors affect the solubility of CS derivatives in aqueous systems dependent on CS. According to previous studies, since the amino groups are converted to -NH-CO- groups in the current

method, only a few groups can be protonated or dissociated in distilled water. Theoretically, the electrostatic interaction is not the most important factor in NSCS/PEO adsorption into FLX. The decrease in the intermolecular H-bonding facilitates NSCS dispersion into solution. In addition to acetyl groups and glycosidic rings, the remaining intermolecular H-bonds and new hydrophobic moieties in NSCS prevent it from dissolving in water and forming a true solution. The poor intermolecular H-bonding caused by the -NH-CO- and -OH groups along the NSCS macromolecular chains, as well as hydrophobic interaction among the hydrophobic moieties in NSCS, such as $-CH_2CH_2$, acetyl groups, and glycosidic rings, are expected to be the driving forces for NSCS/PEO nanofiber adsorption in water (Zhu *et al*. 2006).

The pH of the media was modified and optimized because high adsorption capacity for NSCS/PEO nanofibers at standard value (5.3) is difficult to achieve. As a result, experiments were conducted at pH 7 to 10, and pH 9.00 was the most effective for adsorption (highest Q_t). The adsorbent had an overall adsorption efficiency of about 71.9 mg/g at the pH of the solution (9.0). On the other hand, the optimum pH was 8.0 because going further than pH 8.5 the membrane became soluble in the medium and was degraded to a greater degree. The relationship between FLX adsorption time and NSCS/PEO adsorption capacities is depicted in Fig. 8. Within 2.5 h at 25 °C, the adsorption potential increased rapidly in the early stages of the reaction. The pseudo-first-order and pseudo-second-order models were used to analyze the experimental data and determine the adsorption kinetics mechanism. Pseudo-first-order rate for FLX sorption on NSCS/PEO nanofibers gave a better correlation than the second-order-rate (coefficient of determination $R^2 = 0.9979$ compared to $R^2 = 0.9769$). According to the mechanism, the rate of FLX adsorption is influenced by the pH of ions at the adsorbent surface. This finding is supported by the fact of the ZP value that resulted in high negative charge surface in basic media. The calculated rate constant k_1 was 0.06764 g/mmol/h. In 45-min, FLX adsorption achieved equilibrium. The effect of time on the adsorption behaviour of FLX by NSCS/PEO nanofibers followed the pseudo-first-order and pseudo-second-order models.

Both models fitted well in most cases, as can be seen in Table 2. It has been reported by many authors in the literature that pseudo-first-order kinetic curves are not appropriate for determining nanofibrous adsorbent kinetics (Gerente et al. 2007). Due to the poor correlation associated with pseudo-first-order, most authors have chosen pseudo-second-order over pseudo-first-order due to the linear equation. This type of adsorption seems to be limited by the reaction between the contaminants and the nanofibers, rather than by contaminant transfer to the adsorbent or diffusion through the membrane, as the adsorption well fitted a pseudo-first-order model. A pseudo-first-order reaction also demonstrates that one of the two factors (adsorbate and adsorbent) is very concentrated. Contaminant concentrations in excess would mean that all nanofiber active sites would be saturated. In contrast, if active sites are more abundant, the pseudo-first-order model would be more fitting since pharmaceutical residues are found in trace concentrations in wastewater.

Based on finding of a ZP measurement of the surface charge of NSCS, the surface charge of NSCS showed a negative charge in the alkaline media, confirming the validity that the adsorption capacity (Q_e) increases gradually as pH level is increased from 6.5 to 9 in the alkaline media. In order to understand how NSCS/PEO nanofibers interact with target drugs (FLX), it's important to understand that FLX normally has a pK_a value of 9.8, which means running NSCS/PEO nanofibers in basic medium at pH > 9.0 will cause no protonation of nitrogen. Therefore, adjustment of the pH at 7 and 8 are the optimum pH

conditions to have attractive side ionic exchange to give stronger bonding. NSCS/PEO nanofibers are presenting a negative ionized form ($pK_{a\text{-}COOH}$ = 4.5), whereas FLX, which is a weak base, has a positive charge protonated on it (pK_a = 9.8). According to ZP measurements of the NSCS/PEO nanofiber mats, the found pH_{iep} was around 6.3, which means that a pH higher than 6.3 should bring high ionization of the surface, thus yielding a higher negative charge. This is expected to lead to greater solubility and degradation in at pH values higher than 9.0, as shown in Fig. 7.

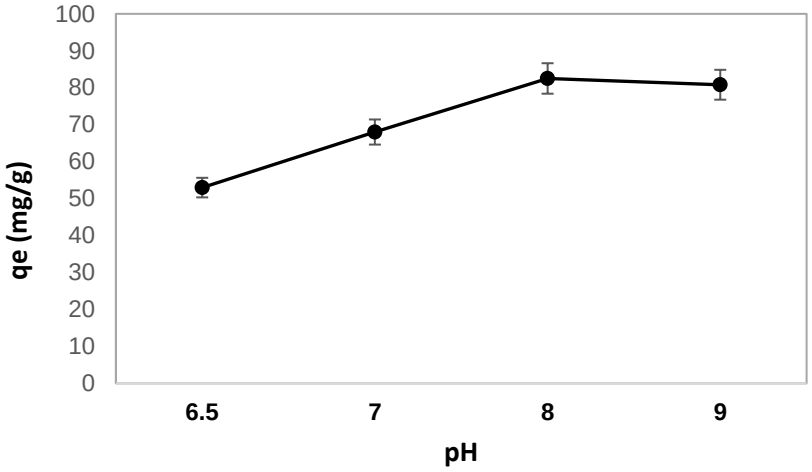

Fig. 7. Effect of pH on the adsorption of FLX onto NSCS/PEO (6:4) nanofibers

Currently, the physical contact controls the processes at the surface of the modified biopolymer in low pH solution (acidic medium). The kinetic experiment will follow the pseudo first order because the described adsorption capacity of FLX is around (Q_e=71.9 mg/g). Many studies have looked at using continuous adsorption to treat drug contaminants because of its benefits, such as high adsorption performance, flexibility, and adsorbent renewal capacity. Furthermore, pharmaceutical residues have a significant environmental impact; thus, their management has been the subject of numerous studies (Ahmed and Hameed 2018). Batch adsorption can handle enormous amounts of drug solution while still achieving excellent removal efficiency. Such a process may also be easily scaled up from a laboratory to an industrial setting (Lemus *et al*. 2017).

Indeed, real-world wastewater contains many toxins that are not separated in nature. To put it another way, they exist in groups and in combination with other pollutants. As a result, there is mounting evidence that the toxicity of medicinal combinations is greater than the toxicity of individual drugs. The adsorption of FLX, VER, CBZ, and IUP to NSCS/PEO nanofibers was studied to learn more about the adsorption mechanism of those pollutants on NSCS/PEO in aqueous solutions. In comparison to the experimental data, our understanding of the adsorption behaviour of numerous pharmaceuticals revealed that the adsorption capacity is reduced relative to what is expected for individual neutral and acidic drugs (*e.g.* CRB and IUP) and increases in the case of a basic drug (*e.g.* FLX and VEX) (Tan *et al.* 2008). Furthermore, drug adsorption is greatly influenced by pH.

Table 3 and Fig. 8 show the results of the experiment for various medications in combination and separately.

Table 3. Experimental for Individual and Parallel Pharmaceuticals Adsorption Capacity

Contaminant	Individual Adsorption Capacity (mg/g)	Individual Adsorption Capacity (mg/g)
Fluoxetine (FLX)	82.11 ± 3.77	33.10 ± 0.15
Venlafaxine (VEN)	54.02 ± 0.31	17.62 ± 1.50
Carbamazepine (CAB)	47.51 ± 2.16	10.24 ± 0.81
Ibuprofen (IBU)	25.98 ± 1.27	4.89 ± 1.99

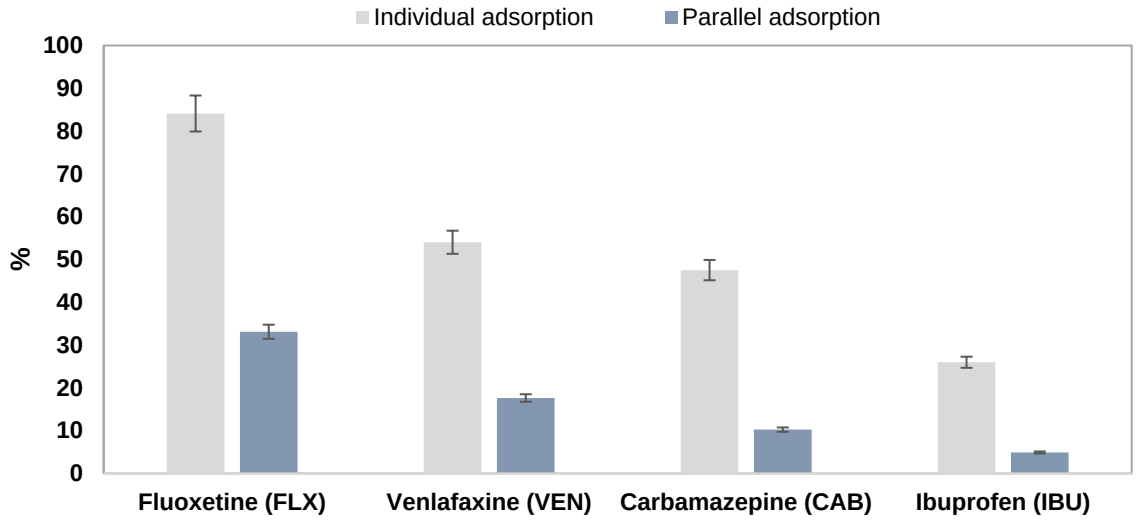

Fig. 8. The adsorption of various medications in single/multiple pharmaceuticals in solution at pH 7 and 25 °C was compared

Different adsorption experiments were carried out using a mixture of four pharmaceuticals (FLX, VEX, CRB, IUP) in 50 ppm concentration for each single pharmaceutical, and multiple pharmaceuticals with 12.5 ppm for each drug to test the influence of the presence of other drugs in the solution on the single adsorption process. As a result, the adsorption capacity of each medication in both systems did not match. As can be seen, single pharmaceuticals had a higher adsorption capacity than multiple pharmaceuticals, implying that in batch adsorption of single pharmaceuticals, the chemical interaction between the adsorbent (NSCS/PEO) and the one pharmaceutical (FLX) as an alkaline drug is more direct, with no specific interactions among the different pharmaceutical compounds. As a result, in the case of one pharmaceutical, the interaction will be strong, whereas in the case of multiple pharmaceuticals, the adsorbent will be unable to bond with the various pharmaceuticals because the four pharmaceuticals have different behaviours and functional groups, making it difficult to form interactions between them. As a result, the chance for the NSCS/PEO to adsorb the pharmaceutical will be reduced.

The NSCS/PEO nanofibers' pharmaceutical adsorption capacities were compared to those of other adsorbents in earlier research, and it was shown that their adsorption capacities were substantially higher than those of other adsorbents (Table 4).

Table 4. Adsorption Capacity Values for the Adsorption of FLX On Different Adsorbents

Adsorbents	Adsorption capacity (mg/g)	References
Mesoporous ferrite nanoparticles of ruthenium ($RuFeO_3$) and cerium ($CeFeO_3$)	729.6 (>99%)	(Narayanan *et al*. 2021)
NSCS/PEO nanofibers	82.3	---
N, O-CMCS/PEO nanofibers	79.7	(Khierallah *et al*. 2021)
Lignin/PVA nanofibers	78.2	(Camiré *et al*. 2020b)
Biochar, rice bran pyrolysis	67.6	(Román *et al*. 2020)
Hydrochar, activated carbons	44.1	(Quiñones et al. 2018)
Biochar, Eucalyptus pyrolysis	6.4	(Escudero-Curiel *et al*. 2021)
β-Cyclodextrin carboxymethyl cellulose (β-CD-CMC) polymer	5.1	(Silva *et al*. 2020)

Desorption Studies

The desorption process and mechanisms of the adsorbed FLX on the NSCS/PEO nanofibers are critical to understanding. Reusing used adsorbents is seen as a key economic factor in cutting down on material prices. For the NSCS/PEO nanofiber, a range of desorption conditionals were investigated, including altering the pH (acidic pH) with different concentrations (0.1, 0.01, and 0.001 M) of HCl and acetic acid (5, 10, and 50%), 100% methanolic solutions, and heating the solution in an ultrasound bath. The desorption procedure took more than two months to complete, making it the most time-consuming part of the study. There were numerous attempts to produce the safest and most optimal desorption conditions. It was determined that a low concentration of HCl boosted the desorption removal capacity in acidic media at pH 3, and that increasing the concentration of HCl and acetic acid led to an increase in the adsorption capacity, but the nanofiber membrane lost too much weight and disintegrated. The NSCS/PEO has total desorption removal capabilities of 71% at pH 2.0 (1% HCl) and 78 % in 10% acetic acid. However, even after numerous cycles, the adsorbent was found to successfully retain FLX.

First, even at low concentrations of the methanolic solution, the amount of desorption of NSCS/PEO nanofibers was too low, in addition to deteriorating, causing the membrane to lose weight too quickly. The solution was then heated in an ultrasonic bath. This helped to desorb the membrane by elevating the temperature, as opposed to the first scenario discussed above. Supporting the heating with ultrasound, on the other hand, resulted in a small increase in desorption. Damaged, degraded, and losing the weight of the adsorbent (NSCS/PEO) mat was the outcome in both cases. As the pH of the solution was elevated, the proportion of NSCS/PEO desorption was reduced drastically, indicating the preferred desorption condition. At pH 5.0, desorption was minimal, while at pH 2.0, the most desorption was recorded. Because substantial desorption was seen at pH 2.0, it was concluded that FLX adsorption on NSCS/PEO is predominantly owing to electrostatic attraction, validating the pH influence on adsorption. To clarify, the principal adsorption interactions of NSCS/PEO nanofibers were electrostatically preferred in many other works. Thus, when the pH was less than 5, the chemical interaction became weak and the electrostatic connection broke, resulting in FLX desorption. Because of that, the desorption of nanofibers NSCS/PEO has not been widely investigated, so more experimental conditions and mechanisms study are needed.

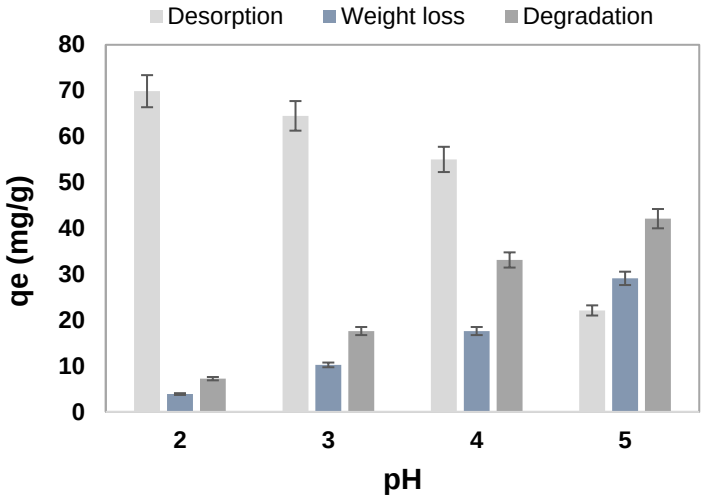

Fig. 9. Various pH experimental conditions on NSCS/PEO (6:4) for desorption solution, weight loss and degradation of the nanofiber membrane

Figure 9 indicates that in basic media, not only was desorption poor but the nanofibers are also degraded, resulting in large weight losses in the nanofibrous. Acidic pH can produce high desorption without significant weight loss. Desorption efficiency rises with decreasing pH to 2.0. Because the electrostatic connections between the NSCS/PEO mat and FLX are decreased in an acidic environment, FLX desorption from the membrane is improved.

For the economic feasibility of adsorbent for water filtration, it is critical to regenerate wasted adsorbent. The regeneration of NSCS/PEO nanofibers was investigated using four adsorption/desorption cycles as shown in Fig. 10. Desorption studies can aid in the understanding of an adsorption process mechanism. If water can desorb the FLX adsorbed on the adsorbent, the FLX is attached to the adsorbent by weak bonds; if strong acids (such as H_2SO_4 and HCl) can desorb the FLX, it is thought that the FLX is attached to the adsorbent via ion exchange or electrostatic attraction (Li *et al*. 2011). As a result, the influence of pH on FLX desorption capacity onto NSCS/PEO nanofibers was tested using distilled water with various pH values. The desorption capacity fell significantly as the pH increased; the lowest desorption capacity was at high pH of up to 7.0 (basic pH), while the highest desorption capacity was at pH 2. The electrostatic attraction had a substantial role in the adsorption of FLX onto the NSCS/PEO nanofibers (Li *et al*. 2011). The adsorbed FLX on NSCS/PEO can be desorbed into the solution at varied concentrations of HCl (1, 0.1, 0.01, and 0.001 M, respectively). The desorption of FLX increased for HCl as the regenerant concentration was increased to 1 M. When acids are utilized as regenerants, the amine functional groups on the sorbents are protonated, causing a repulsive force between the adsorbed FLX and the $-NH_3^+$ groups, resulting in FLX being released into the solution (Kannamba *et al*. 2010).

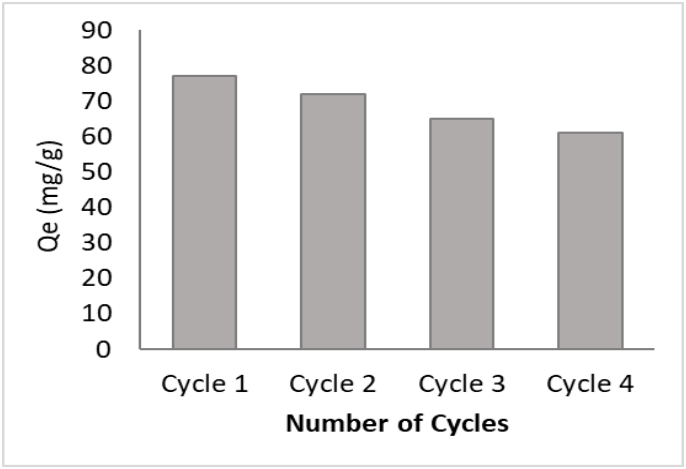

Fig. 10. Desorption cycles of NSCS/PEO (6:4) for fluoxetine using 1M HCl (pH 2)

CONCLUSIONS

1. In this study project, an innovative modified chitosan (CS) nanomaterial was developed using an electrospinning method to adsorb pharmaceutical residues in water. The synthesis of N-succinyl chitosan (NSCS) was successful, a well-designed biocompatible CS derivative. NSCS/poly(ethylene oxide) (PEO) nanofibers are promising adsorbents for fluoxetine (FLX) removal from water. On the basis of Fourier transform infrared (FTIR) and proton nuclear magnetic resonance (^{1}H-NMR) results, NSCS structure was successfully manufactured and verified.
2. This eco-friendly material with an average diameter of 183 ± 38 nm is a promising adsorbent to replace activated carbon (AC). For electrospinning, different ratios of NSCS and PEO were tried to find the optimal nanofiber for adsorption of FLX was at concentration (8 wt%/5 wt%) (6:4 mass ratio) as a model of pollutants in aqueous solution.
3. Batch adsorption investigations revealed that the NSCS/PEO adsorption capability for FLX elimination was highly dependent on the starting pH based on zeta-potential results. The pseudo-second-order model accurately represented the FLX adsorption equilibrium on NSCS/PEO mats, according to the kinetics studies. NSCS/PEO achieved the highest percentage removals at a pH value of 8.0, with a maximum adsorption capacity up to 82.3 ± 3.4 mg/g for FLX.
4. Repeated adsorption-desorption cycles showed this sorbent material's remarkable reusability potential, making it appropriate for water purification.
5. In all tests, purified water was used as a matrix. Hence, it would be interesting, in future work, to determine whether satisfactory adsorption results can be obtained in urine or wastewater. In spite of the fact that a great deal of work has been accomplished, many points need improvement or cannot be addressed. In the future, the project will examine dynamic adsorption tests to allow continuous water treatment. Consequently, the authors would like to test and evaluate the adsorption efficiency of sorbent media developed in this study on real wastewater from typical industries, such as mining and pharmaceuticals.

6. To contribute to this long-term goal, the results of this study will be used to establish the critical parameters for industrial equipment for tertiary treatment.
7. The adsorption isotherm test is a great idea. Still, time constraints and the difficulty of obtaining a sufficient amount of nanofiber materials (membranes) by electrospinning made it impossible to complete the isotherm test. The isotherm test will be performed in the near future.

ACKNOWLEDGMENTS

The authors gratefully acknowledge Professor Eric Loranger from Université du Québec à Trois-Rivières for his helpful advice and assistance. Jean-Philippe Marineau and Jocelyn Bouchard are also acknowledged for their technical assistance, as well as Agnès Lejeune for SEM images, Heidi Levasseur for language assistance, and the Libyan-North American Scholarship Program (LNASP), the Canadian Bureau for International Education (CBIE) for financial support.

REFERENCES CITED

Ahmed, M. J., and Hameed, B. H. (2018). "Removal of emerging pharmaceutical contaminants by adsorption in a fixed-bed column: A review," *Ecotoxicology and Environmental Safety* 149 (December 2017), 257-266. DOI: 10.1016/j.ecoenv.2017.12.012

Ali, I., Asim, M., and Khan, T. A. (2012). "Low cost adsorbents for the removal of organic pollutants from wastewater," *Journal of Environmental Management* 113, 170-183. DOI: 10.1016/j.jenvman.2012.08.028

Angammana, C. J., and Jayaram, S. H. (2016). "Fundamentals of electrospinning and processing technologies," *Particulate Science and Technology* 34(1), 72-82. DOI: 10.1080/02726351.2015.1043678

Bashir, S., Teo, Y. Y., Naeem, S., Ramesh, S., and Ramesh, K. (2017). "Correction: pH responsive N-succinyl chitosan/poly (acrylamide-co-acrylic acid) hydrogels and in vitro release of 5-fluorouracil (PLoS ONE (2017) 12:7 (E0179250) DOI: 10.1371/Journal.Pone.0179250)," *PLoS ONE* 12(9), 1-24. DOI: 10.1371/journal.pone.0185505

Bashir, S., Teo, Y. Y., Ramesh, S., and Ramesh, K. (2016). "Synthesis, characterization, properties of N-succinyl chitosan-g-poly (methacrylic acid) hydrogels and in vitro release of theophylline," *Polymer* 92, 36-49. DOI: 10.1016/j.polymer.2016.03.045

Bashir, S., Teo, Y. Y., Ramesh, S., and Ramesh, K. (2017). "Physico-chemical characterization of pH-sensitive N-succinyl chitosan-g-poly (acrylamide-co-acrylic acid) hydrogels and in vitro drug release studies," *Polymer Degradation and Stability* 139, 38-54. DOI: 10.1016/j.polymdegradstab.2017.03.014

Brasselet, C., Pierre, G., Dubessay, P., Dols-Lafargue, M., Coulon, J., Maupeu, J., Vallet-Courbin, A., de Baynast, H., Doco, T., Michaud, P., and Delattre, C. (2019). "Modification of chitosan for the generation of functional derivatives," *Applied Sciences (Switzerland)* 9(7), 1321. DOI: 10.3390/app9071321

Camiré, A., Espinasse, J., Chabot, B., and Lajeunesse, A. (2020a). "Development of

electrospun lignin nanofibers for the adsorption of pharmaceutical contaminants in wastewater," *Environmental Science and Pollution Research* 27 (4), 3560-3573. DOI: 10.1007/s11356-018-3333-z

Camiré, A., Espinasse, J., Chabot, B., and Lajeunesse, A. (2020b). "Development of electrospun lignin nanofibers for the adsorption of pharmaceutical contaminants in wastewater," *Environmental Science and Pollution Research* 27 (4), 3560-73. DOI: 10.1007/s11356-018-3333-z

Celebioglu, A., and Uyar, T. (2013). "Electrospinning of nanofibers from non-polymeric systems: Electrospun nanofibers from native cyclodextrins," *Journal of Colloid and Interface Science* 404, 1-7. DOI: 10.1016/j.jcis.2013.04.034

Cevallos-Mendoza, J., Amorim, C. G., Rodrizuez-Diaz, J. M., and Montenegro, M. C. B. S. M. (2022). "Removal of contaminants from water by membrane filtration: A review," *Membranes* 12(6), 1-23. DOI: 10.3390/membranes12060570

Chaudhry, F. N., and Malik, M. F. (2017). "Factors affecting water pollution: A review," *Journal of Ecosystem & Ecography* 07 (01), 5-8. DOI: 10.4172/2157-7625.1000225

Chen, F. M., and Liu, X. (2016). "Advancing biomaterials of human origin for tissue engineering," *Progress in Polymer Science* 53, 86-168. DOI: 10.1016/j.progpolymsci.2015.02.004

Cheung, R. F. C., Ng, T. B., Wong, J. H., and Chan, W. Y. (2015). "Chitosan: An update on potential biomedical and pharmaceutical applications," *Mar. Drugs* 13(8), 5156-5186. DOI: 10.3390/md13085156

Duan, B., Dong,C., Yuan, X., and Yao, K. (2004). "Electrospinning of chitosan solutions in acetic acid with poly(ethylene oxide)," *Journal of Biomaterials Science, Polymer Edition* 15(6), 797-811. DOI: 10.1163/156856204774196171

Ebele, A. J., Abdallah, M. A. E., and Harrad, S. (2017a). "Pharmaceuticals and personal care products (PPCPs) in the freshwater aquatic environment," *Emerging Contaminants* 3(1), 1-16. DOI: 10.1016/j.emcon.2016.12.004

Ebele, A. J., Abdallah, M. A. E., and Harrad, S. (2017b). "Pharmaceuticals and personal care products (PPCPs) in the freshwater aquatic environment," *Emerging Contaminants* 3(1), 1-16. DOI: 10.1016/j.emcon.2016.12.004

Erickson, M. L., Langer, S. K., Roth, J. L., and Kroening, S. E. (2014). *Contaminants of Emerging Concern in Ambient Groundwater in Urbanized Areas of Minnesota, 2009-12*, U.S. Geological Survey, Reston, VA, USA.

Escudero-Curiel, S., Acevedo-García, V., Ángeles Sanromán, M., and Pazos, M. (2021). "Eco-approach for pharmaceutical removal: Thermochemical waste valorisation, biochar adsorption and electro-assisted regeneration," *Electrochimica Acta* 389, article 138694. DOI: 10.1016/j.electacta.2021.138694

Ferronato, N., and Torretta, V. (2019). "Waste mismanagement in developing countries: A review of global issues," *International Journal of Environmental Research and Public Health* 16(6), 1060. DOI: 10.3390/ijerph16061060

Gabelman, A. (2017). "Adsorption basics: Part 2," *Chemical Engineering Progress* 113(8), 1-6.

Gerente, C., Lee, V. K. C., Le Cloirec, P., and McKay, G. (2007). "Application of chitosan for the removal of metals from wastewaters by adsorption – Mechanisms and models review," *Critical Reviews in Environmental Science and Technology* 37(1), 41-127. DOI: 10.1080/10643380600729089

Giri, T. K., Thakur, A., Alexander, A., Ajazuddin, Badwaik, H., and Tripathi, D. K. (2012). "Modified chitosan hydrogels as drug delivery and tissue engineering

systems: Present status and applications," *Acta Pharmaceutica Sinica B* 2(5), 439-449. DOI: 10.1016/j.apsb.2012.07.004

Gomes, J., Costa, R., Quinta-Ferreira, R. M., and Martins, R. C. (2017). "Application of ozonation for pharmaceuticals and personal care products removal from water," *Science of the Total Environment* 586, 265-283. DOI: 10.1016/j.scitotenv.2017.01.216

Guibal, E. (2004). "Interactions of metal ions with chitosan-based sorbents: A review," *Separation and Purification Technology* 38(1), 43-74. DOI: 10.1016/j.seppur.2003.10.004

Hamdaoui, O. (2006). "Batch study of liquid-phase adsorption of methylene blue using cedar sawdust and crushed brick," *Journal of Hazardous Materials* 135(1-3), 264-273. DOI: 10.1016/j.jhazmat.2005.11.062

Hernandez-Ramirez, O., and Holmes, S. M. (2008). "Novel and modified materials for wastewater treatment applications," *Journal of Materials Chemistry* 18(24), 2751-2761. DOI: 10.1039/b716941h

Howard, G., and Bartram, J. (2010). *Vision 2030: The Resilience of Water Supply and Sanitation in the Face of Climate Change: Technical Report*, World Health Organization, Geneva, Switzerland.

Kamaz, M., Wickramasinghe, S. R., Eswaranandam, S., Zhang, W., Jones, S. M., Watts, M. J., and Qian, X. (2019). "Investigation into micropollutant removal from wastewaters by a membrane bioreactor," *International Journal of Environmental Research and Public Health* 16(8). DOI: 10.3390/ijerph16081363

Kamoun, E. A. (2016). "N-Succinyl chitosan-dialdehyde starch hybrid hydrogels for biomedical applications," *Journal of Advanced Research* 7(1), 69-77. DOI: 10.1016/j.jare.2015.02.002

Kannamba, B., Reddy, K. L., and AppaRao, B. V. (2010). "Removal of Cu(II) from aqueous solutions using chemically modified chitosan," *Journal of Hazardous Materials* 175(1-3), 939-48. DOI: 10.1016/j.jhazmat.2009.10.098

Kato, Y., Onishi, H., and Machida, Y. (2001). "Lactosaminated and intact N-succinyl-chitosans as drug carriers in liver metastasis," *International Journal of Pharmaceutics* 226(1-2), 93-106. DOI: 10.1016/S0378-5173(01)00777-3

Khierallah, A. H. I., Bates, I. I. C., Chabot, B., and Lajeunesse, A. (2021). "Adsorption of pharmaceutical contaminants from aqueous solutions using N,O-carboxymethyl chitosan/polyethylene oxide (PEO) electrospun nanofibers," *Journal of Materials Science and Chemical Engineering* 09(11), 15-38. DOI: 10.4236/msce.2021.911003

Kyzas, G. Z., and Bikiaris, D. N. (2015). "Recent modifications of chitosan for adsorption applications: A critical and systematic review," *Marine Drugs* 13(1), 312-37. DOI: 10.3390/md13010312

Kyzas, G. Z., Bikiaris, D. N., Seredych, M., Bandosz, T. J., and Deliyanni, E. A. (2014a). "Removal of dorzolamide from biomedical wastewaters with adsorption onto graphite oxide/poly(acrylic acid) grafted chitosan nanocomposite," *Bioresource Technology* 152, 399-406. DOI: 10.1016/j.biortech.2013.11.046

Kyzas, G. Z., Bikiaris, D. N., Seredych, M., Bandosz, T. J., and Deliyanni, E. A. (2014b). "Removal of dorzolamide from biomedical wastewaters with adsorption onto graphite oxide/poly(acrylic acid) grafted chitosan nanocomposite," *Bioresource Technology* 152, 399-406. DOI: 10.1016/j.biortech.2013.11.046

Li, Q., Zhao, Y.-H., Wang, L., and Wang, A.-Q. (2011). "Adsorption characteristics of methylene blue onto the N-succinyl-chitosan-g-polyacrylamide/attapulgite

composite," *Korean Journal of Chemical Engineering* 28(8), 1658-1664. DOI: 10.1007/s11814-011-0037-1

Li, X., Wang, Y., Li, A., Ye, Y., Peng, S., Deng, M., and Jiang, B. (2019). "A novel pH- and salt-responsive N-succinyl-chitosan hydrogel via a one-step hydrothermal process," *Molecules* 24(23), article 4211. DOI: 10.3390/molecules24234211

Lu, B., Sun, Y.-X., Li, Y.-Q., Zhang, X.-Z., and Zhuo, R. X. (2009). "N-Succinyl-chitosan grafted with low molecular weight polyethylenimine as a serum-resistant gene vector," *Molecular BioSystems* 5(6), 629-37. DOI: 10.1039/b822505b

Lu, S., Song, X., Cao, D., Chen, Y., and Yao, K. (2004). "Preparation of water-soluble chitosan," *Journal of Applied Polymer Science* 91(6), 3497-3503. DOI: 10.1002/app.13537

de Lima, E. L., Vasconcelos, N. F., da Silva Maciel, J., Andrade, F. K., Vieira, R. S., and Andrade Feitosa, J. P. (2020). "Injectable hydrogel based on dialdehyde galactomannan and n-succinyl chitosan: A suitable platform for cell culture," *Journal of Materials Science: Materials in Medicine* 31(1). DOI: 10.1007/s10856-019-6343-6

Min, L.-L., Zhong, L.-B., Zheng, Y.-M., Liu, Q., Yuan, Z.-H., and Yang, L.-M. (2016). "Functionalized chitosan electrospun nanofiber for effective removal of trace arsenate from water," *Scientific Reports* 6(August). DOI: 10.1038/srep32480

Miranda, M. E., S., Marcolla, C., Rodriguez, C. A., Wilhelm, H. M., Sierakowski, M. R., Bresolin, T. M. B., and Alves de Freitas, R. (2006). "I . The role of N-carboxy-methylation of chitosan in the thermal stability and dynamic," *Polym. Int.* 55 (June), 961-069. DOI: 10.1002/pi

Mohammed, Mageed, Rasheed. (2013). "Adsorption techniques for the removal of organic pollutants from water and waste water," *Organic Pollutants-Monitoring, Risk and Treatment*, 167-94.

Monsalve, Y., Sierra, L., and López, B. L. (2015). "Preparation and characterization of succinyl-chitosan nanoparticles for drug delivery," *Macromolecular Symposia* 354 (1), 91-98. DOI: 10.1002/masy.201400128

Mourya, V. K., and Inamdar, N. N. (2008). "Chitosan-modifications and applications: Opportunities galore," *Reactive and Functional Polymers* 68(6), 1013-1051. DOI: 10.1016/j.reactfunctpolym.2008.03.002

Mura, C., Nácher, A., Merino, V., Merino-Sanjuan, M., Carda, C., Ruiz, A., Manconi, M., Loy, G., Fadda, A. M., and Diez-Sales, O. (2011). "N-Succinyl-chitosan systems for 5-aminosalicylic acid colon delivery: In vivo study with TNBS-induced colitis model in rats," *International Journal of Pharmaceutics* 416(1), 145-154. DOI: 10.1016/j.ijpharm.2011.06.025

Naghizadeh, A., and Nabizadeh, R. (2016). "Removal of Reactive Blue 29 dye by adsorption on modified chitosan in the presence of hydrogen peroxide," *Environment Protection Engineering* 42(1), 149-168. DOI: 10.5277/epe160112

Narayanan, J., Hernández, J. G., Padilla-Martínez, I. I., Thangarasu, P., Santos Garay, S. E, Cabrera, C. B. P., and Cuevas, A. J. S. (2021). "Geometry influenced adsorption of fluoxetine over the surface of $RuFeO_3$ and $CeFeO_3$ nanoparticles: Kinetics and thermodynamic studies," *Ceramics International* 47 (14), 20544-20561. DOI: 10.1016/j.ceramint.2021.04.064

Niu, X., Zhu, L., Xi, L., Guo, L., and Wang, H. (2020). "An antimicrobial agent prepared by N-succinyl chitosan immobilized lysozyme and its application in strawberry preservation," *Food Control* 108 (April 2019), article 106829. DOI: 10.1016/j.foodcont.2019.106829

OECD. (2019). "Pharmaceutical residues in freshwater," *OECD Studies on Water*, 136. https://www.oecd-ilibrary.org/environment/pharmaceutical-residues-in-freshwater_c936f42d-en.

Oulton, R. L., Kohn, T., and Cwiertny, D. M. (2010). "Pharmaceuticals and personal care products in effluent matrices: A survey of transformation and removal during wastewater treatment and implications for wastewater management," *Journal of Environmental Monitoring* 12(11), 1956-1978. DOI: 10.1039/c0em00068j

Paradis-Tanguay, L., Camiré, A., Renaud, M., and Chabot, B. (2018). "Sorption capacities of chitosan / polyethylene oxide (PEO) electrospun nanofibers used to remove ibuprofen in water,"

Patel, M., Kumar, R., Kishor, K., Mlsna, T., Pittman, C. U., and Mohan, D. (2019). "Pharmaceuticals of emerging concern in aquatic systems: Chemistry, occurrence, effects, and removal methods," *Chemical Reviews* 119(6), 3510-3673. DOI: 10.1021/acs.chemrev.8b00299

Pereira, I. C., Duarte, A. S., Neto, A. S., and Ferreira, J. M. F. (2019). "Chitosan and polyethylene glycol based membranes with antibacterial properties for tissue regeneration," *Materials Science and Engineering C* 96(November 2018), 606-615. DOI: 10.1016/j.msec.2018.11.029

Quiñones, J. P., Peniche, H., and Peniche, C. (2018). "Chitosan based self-assembled nanoparticles in drug delivery," *Polymers* 10(3), 1-32. DOI: 10.3390/polym10030235

Román, S., Nabais, J. M. V., Ledesma, B., Laginhas, C., and Titirici, M. M. (2020). "Surface interactions during the removal of emerging contaminants by hydrochar-based adsorbents," *Molecules* 25(9), 1-12. DOI: 10.3390/molecules25092264

Shariatinia, Z., and Jalali, A. M. (2018). "Chitosan-based hydrogels: Preparation, properties and applications," *International Journal of Biological Macromolecules* 115, 194-220. DOI: 10.1016/j.ijbiomac.2018.04.034

Silva, B., Martins, M., Rosca, M., Rocha, V., Lago, A., Neves, I. C., and Tavares, T. (2020). "Waste-based biosorbents as cost-effective alternatives to commercial adsorbents for the retention of fluoxetine from water," *Separation and Purification Technology* 235(September 2019), 116139. DOI: 10.1016/j.seppur.2019.116139

Skorik, Y. A., Kritchenkov, A. S., Moskalenko, Y. E., Golyshev, A. A., Raik, S. R., Whaley, A. K., Vasina, L. V., and Sonin, D. L. (2017). "Synthesis of N-succinyl- and N-glutaryl-chitosan derivatives and their antioxidant, antiplatelet, and anticoagulant activity," *Carbohydrate Polymers* 166, 166-172. DOI: 10.1016/j.carbpol.2017.02.097

Sun, J., Xiao, C., Tan, H., and Hu, X. (2013). "Covalently crosslinked hyaluronic acid-chitosan hydrogel containing dexamethasone as an injectable scaffold for soft tissue engineering," *Journal of Applied Polymer Science* 129(2), 682-688. DOI: 10.1002/app.38779

Sun, S., and Wang, A. (2006a). "Adsorption kinetics of Cu(II) ions using N,O-carboxymethyl-chitosan," *Journal of Hazardous Materials* 131(1-3), 103-111. DOI: 10.1016/j.jhazmat.2005.09.012

Sun, S., and Wang, A. (2006b). "Adsorption properties of N-succinyl-chitosan and cross-linked N-succinyl-chitosan resin with Pb(II) as template ions," *Separation and Purification Technology* 51(3), 409-415. DOI: 10.1016/j.seppur.2006.03.004

Tan, H., Chu, C. R., Payne, K. A., and Marra, K. G. (2009). "Injectable in situ forming biodegradable chitosan-hyaluronic acid based hydrogels for cartilage tissue engineering," *Biomaterials* 30(13), 2499-2506. DOI: 10.1016/j.biomaterials.2008.12.080

Tan, I. A.W., Ahmad, A. L., and Hameed, B. H. (2008). "Adsorption of basic dye on high-surface-area activated carbon prepared from coconut husk: Equilibrium, kinetic and thermodynamic studies," *Journal of Hazardous Materials* 154(1-3), 337-346. DOI: 10.1016/j.jhazmat.2007.10.031

Tapdigov, S. Z. (2021). "The bonding nature of the chemical interaction between trypsin and chitosan based carriers in immobilization process depend on entrapped method: A review," *International Journal of Biological Macromolecules* 183, 1676-1696. DOI: 10.1016/j.ijbiomac.2021.05.059

Vakili, M., Rafatullah, M., Salamatinia, B., Zuhairi, A., Hakimi, M., Bing, K., Gholami, Z., and Amouzgar, P. (2014). "Application of chitosan and its derivatives as adsorbents for dye removal from water and wastewater: A review," *Carbohydrate Polymers* 113, 115-130. DOI: 10.1016/j.carbpol.2014.07.007

Wang, L., and Wang, A. (2008). "Adsorption behaviors of Congo Red on the N,O-carboxymethyl-chitosan/montmorillonite nanocomposite," *Chemical Engineering Journal* 143(1-3), 43-50. DOI: 10.1016/j.cej.2007.12.007

Williams, G. R., Raimi-Abraham, B. T., and Luo, C. J. (2018). *Nanofibres in Drug Delivery*, UCL Press, London. DOI: 10.14324/111.9781787350182

Zhang, C. G., Zhu, Q. L., Zhou, Y., Liu, Y., Chen, W. L., Yuan, Z. Q., Yang, S. D., Zhou, X. F., Zhu, A. J., Zhang, X. N., and Jin, Y. (2014). "N-Succinyl-chitosan nanoparticles coupled with low-density lipoprotein for targeted osthole-loaded delivery to low-density lipoprotein receptor-rich tumors," *International Journal of Nanomedicine* 9(1), 2919-2932. DOI: 10.2147/IJN.S59799

Zhang, Q. Q., Ying, G. G., Pan, C, G., Liu, Y. S., and Zhao, J. L. (2015). "Comprehensive evaluation of antibiotics emission and fate in the river basins of china: source analysis, multimedia modeling, and linkage to bacterial resistance," *Environmental Science and Technology* 49(11), 6772-6782. DOI: 10.1021/acs.est.5b00729.

Zhou, J. Q., and Wang, J. W. (2009). "Immobilization of alliinase with a water soluble-insoluble reversible N-succinyl-chitosan for allicin production," *Enzyme and Microbial Technology* 45(4), 299-304. DOI: 10.1016/j.enzmictec.2009.07.007

Zhou, X., Shi, G., Fan, B., Cheng, X., Zhang, X., Wang, X., Liu, S., Hao, Y., Wei, Z., Wang, L. Y., and Feng, S. Q. (2018). "Polycaprolactone electrospun fiber scaffold loaded with IPSCs-NSCs and ASCs as a novel tissue engineering scaffold for the treatment of spinal cord injury," *International Journal of Nanomedicine* 13, 6265-6277. DOI: 10.2147/IJN.S175914

Zhu, A.-P., Chen, T., Yuan, L.-H., Wu, H., and Lu, P. (2006). "Synthesis and characterization of N-succinyl-chitosan and its self-assembly of nanospheres," *Carbohydrate Polymers* 66(2), 274-279. DOI: 10.1016/j.carbpol.2006.03.014

Ziylan, A., and Ince, N. H. (2011). "The occurrence and fate of anti-inflammatory and analgesic pharmaceuticals in sewage and fresh water: Treatability by conventional and non-conventional processes," *Journal of Hazardous Materials* 187 (1-3), 24-36. DOI: 10.1016/j.jhazmat.2011.01.057

Article submitted: November 22, 2022; Peer review completed: December 21, 2022; Revised version received: January 16, 2023; Accepted: January 17, 2023; Published: January 25, 2023.
DOI: 10.15376/biores.18.1.1971-1998